Metabolic Brain Disease
https://doi.org/10.1007/s11011-019-00396-2

ORIGINAL ARTICLE

Neuroprotective effect of grape seed extract on brain ischemia: a proteomic approach

Safwen Kadri[1] · Mohamed El Ayed[1] · Pascal Cosette[2] · Thierry Jouenne[2] · Salem Elkhaoui[1] · Sami Zekri[3] · Ferid Limam[1] · Ezzedine Aouani[1] · Meherzia Mokni[1]

Received: 29 October 2018 / Accepted: 4 February 2019

Abstract

Stroke is one of the leading causes of long-lasting disability in human and oxidative stress an important underlying cause. Molecular insights into pathophysiology of ischemic stroke are still obscure, and the present study investigated the protective effect of high dosage Grape Seed Extract (GSE 2.5 g/kg) on brain ischemia-reperfusion (I/R) injury using a proteomic approach. Ischemia was realized by occlusion of the common carotid arteries for 30 min followed by 1 h reperfusion on control or GSE pre-treated rats, and a label-free quantification followed by mass spectrometry analysis used to evaluate I/R induced alterations in protein abundance and metabolic pathways as well as the protection afforded by GSE. I/R-induced whole brain ionogram dyshomeostasis, ultrastructural alterations, as well as inflammation into hippocampal dentate gyrus area, which were evaluated using ICP-OES, transmission electron microscopy and immuno-histochemistry respectively. I/R altered the whole brain proteome abundance among which 108 proteins were significantly modified (35 up and 73 down-regulated proteins). Eighty-four proteins were protected upon GSE treatment among which 27 were up and 57 down-regulated proteins, suggesting a potent protective effect of GSE close to 78%of the disturbed proteome. Furthermore, GSE efficiently prevented the brain from I/R-induced ion dyshomeostasis, ultrastructural alterations, inflammatory biomarkers as CD56 or CD68 and calcium burst within the hippocampus. To conclude, a potent protective effect of GSE on brain ischemia is evidenced and clinical trials using high dosage GSE should be envisaged on people at high risk for stroke.

Keywords Stroke · Ischemia-reperfusion · Grape seed extract · Proteomics · Neuroprotection

Introduction

Ischemic stroke is a leading cause of death and long lasting disability worldwide that occurred following the obstruction or diminution of blood flow supply to specific brain areas. Up to now there is no satisfactory therapy and most of the clinical treatments failed to improve the stroke outcome (Doyle et al. 2008). Ischemic insult induces a wide array of early events including excitotoxicity, inflammation, free radical production and ions dyshomeostasis in the ischemic core leading to cell death. Excitotoxicity is triggered by Ca^{2+} burst along with ATP depletion and failure of Na^{+}/K^{+}ATPases leading to membrane depolarization, glutamate accumulation into the extracellular space and opening of NMDA associated Ca^{2+}channels. The burst in calcium triggers the activation of destructive enzymes such as calpains or lipases, which in turn induce the release of pro-inflammatory cytokines and cellular mediators such as NO which interacts with free radicals to induce highly toxic peroxynitrite (Sharipov et al. 2014), a powerful free radical capable of inducing severe lipoperoxidation into the brain, highly prone to oxidative stress due to its low anti-oxidative defence and high polyunsaturated fatty acids content (Pacher et al. 2007).

GSE is a natural and complex mixture of bioactive polyphenolic compounds such as flavonoids, non flavonoids, stilbenes and anthocyanins (Nassiri-Asl and Hosseinzadeh 2009). GSE exhibits a large spectrum of pharmacological

✉ Safwen Kadri
kadri_safwen@live.fr

[1] Bioactive Substances Laboratory, Biotechnology Centre, TechnopolisBorj-Cedria, BP-901, 2050 Hammam-Lif, Tunis, Tunisia

[2] Plateforme Protéomique PISSARO, Institut de Recherche et d′ Innovation Biomédicale, Normandie Université, Mont Saint Aignan, France

[3] Common Services Unit on Transmission Electron Microscopy, Faculty of Medicineof Tunis, University of Tunis El Manar, Bab Saâdoun, Tunis, Tunisia

Published online: 22 February 2019

and multi-organ protective effects such as anti-inflammatory (Chao et al. 2011), and anti-oxidative (Dogan and Celik 2012) as well as liver (Sehirli et al. 2008), brain (Kadri et al. 2015), heart (Mokni et al. 2012) and lung protection (Khazri et al. 2016).

Proteomics, which has the potential to contribute significantly to medical research, is useful for identifying multiple pathogenesis and their progression as stroke. Qualitative label-free LC-MS based proteome analysis has increased drastically over the past decade as a result of technological advances including improvement in sample preparation, database searching and bioinformatics tools that facilitate data interpretation (Lindsey et al. 2015).

In a previous work we showed that GSE protected rat brain from I/R insult mainly through its anti-oxidative properties (Kadri et al. 2015). In the present study, using a high resolution orbitrap LC-MS/MS based proteomic approach we analyzed the effect of I/R on protein abundances, ontologies and pathways as well as the prevention afforded by GSE treatment.

Material and methods

Reagents

GSE was processed from the grape cultivar carignan of *Vitis vinifera* from northern Tunisia. Seeds were air dried and separately grounded using an electric mincer (FP3121 Moulinex) until an ultrafine powder was obtained and dissolved in 10% ethanol (*v*/v) and after vigorous shaking (30 min) and centrifugation (10,000 g, 15 min, 4 °C) supernatant containing soluble polyphenols was used. Composition of GSE was given elsewhere (Charradi et al. 2012).

Animals and treatment

Male Wistar rats (206–226 g) from Pasteur Institute Tunis, were used in accordance with the Ethic Committee of Tunis University and NIH guidelines (Institute of Laboratory Animal Resources (U.S.). Committee on Care and Use of Laboratory Animals., National Institutes of Health (U.S.). Division of Research Resources 1985). They were provided with food and water ad libitum and maintained in animal house at fixed temperature of 22 °C + _ 2 °C with a 12 h light–dark cycle. Rats were randomly divided into three groups of six animals each and daily treated with GSE (2.5 g/kg) by intraperitoneal (ip) route for one week. Such a GSE dosage was chosen according to previous dose response experiments demonstrating the safety and efficiency of varying GSE doses (Charradi et al. 2018).

Group I: Control (C)
Group II: I/R (I)
Group III: GSE + I/R (GI)

Induction of brain I/R injury

At the end of the treatment period, brain I/R was collectively carried out according to (Ueda et al. 2000) at 9 h a.m. to avoid circadian rhythms fluctuations. Briefly, rats were anesthetized with urethane (200 mg/kg) and both common carotid arteries were dissected and clamped for 30 min followed by one hour reperfusion. Animals were then subjected to transcardiac perfusion with NaCl solution (0.9%), brain rapidly excised and homogenized using phosphate buffer saline pH 7.4 with an ultrathuraxT25 homogenizator and sonicated (3x 10s). After centrifugation at 10000 g for15 min at 4 °C, supernatant was used for protein extraction.

Brain protein extraction and in gel digestion

Brain proteins were extracted using bicarbonate buffer 50 mM containing 50 mM DTT and 1% SDS at 55 °C for 15 min and then loaded on 12% polyacrylamide gel. After migration, the gel was incubated in a fixative solution for 30 min, stained with colloidal coomassie brilliant blue overnight and destained after extensive washing with distilled deionized water. The gel was cut into pieces that were washed with 300 μL of distilled deionized water for 15 min, 300 μL of ACN for 15 min and 300 μL of NH_4HCO_3 100 mM pH 8 for 15 min, then a mixture of 300 μL of NH_4HCO_3/ACN (1:1; *v*/v) for 15 min and 300 μL of ACN for 5 min. Band pieces were dried in a speedvac for 5 min, reduction of cysteine residues achieved with 50 μL of 10 mM DTT in NH_4HCO_3 100 mM (pH 8) and gel pieces incubated at 56 °C for1h. Alkylation of cysteine residues was realized using 50 mM iodoacetic acid in 100 mM NH_4HCO_3 pH 8 for 30 min at room temperature in the dark. Band pieces were washed a second time with 300 μL NH_4HCO_3 100 mM pH 8 for 15 min, then incubated in 300 μL NH_4HCO_3/ACN (1:1; *v*/v) mixture for 15 min followed by 5 min incubation in 300 μL ACN and dried in a Speedvac for 5 min. Proteins embedded into band pieces were subjected to tryptic digestion (trypsin 12.5 μg/mL) in NH_4HCO_3 20 mM pH 8 at 37 °C overnight. Peptides were then extracted two times using 1% TFA for 20 min then with 150 μL ACN for 10 min on a shaking platform and then dried into a speedvac.

Nano LC-MS/MS

All analyses were conducted on a LTQ-Orbitrap Elite (Thermo Scientific) coupled with an Easy nLC II system (Thermo Scientific) and nano LC-MS/MS repeated twice. Peptide sample was re-suspended in 10 μL 1% TFA and 4 μL were injected into an enrichment column (C18 PepMap100, Thermo Scientific) and separation achieved with an analytical column needle (NTCC-360/100–5-153, NikkyoTechnos, Japan). The mass spectrometer was used in

positive ionization mode with a capillary voltage and a source temperature set at 1.5 kV and 275 °C, respectively. For protein identification, peptides were analyzed by collision induced dissociation (CID) method and the first scan (MS spectra) was recorded in the Orbitrap analyzer (R = 60.000) at a mass range m/z 400–2000. Then, the 20 most intense ions were selected for MS2 experiments and singly charged species were excluded for MS2 analysis. Dynamic exclusion of already fragmented precursor ions was applied for 30 s, with one repeat count, a repeat duration of 30 s, and an exclusion mass width of ±10 ppm. Fragmentation occurred in the linear ion trap analyzer with collision energy of 35 eV. A target of 5000 ions and a maximum injection time of 200 ms were used for CID MS2 spectra. The method was set to analyze the 20 most intense ions from the survey scan and dynamic exclusion was enabled for 20s. All measurements with the orbitrap analyzer were performed using on-the-fly internal recalibration.

Data analyses

Tandem mass spectra were processed with Thermo Scientific Proteome Discoverer software version 1.3 (Thermo fisher Scientific). Peak lists were determined using the MASCOT engine (Matrix Science version 2.3) and the *Rattus norvegicus* database and SEQUEST® algorithm. The parent-ion and daughter-ion tolerances were 10 ppm and 0.5 Da respectively and peptides filtered based on a false discovery rate (FDR) of 1%.

Label free quantification

The Progenesis LC-MS software from nonlinear dynamics (Newcastle upon Tyne, U.K.) was used to perform label-free quantification. The thermo raw files were loaded onto Progenesis LC-MS software (version 1.0.0.1), aligned automatically, and the resulting aggregate spectrum filtered to include +1, + 2, and + 3 charge state. Protein identification was accepted if established for at least 2 identified peptides. Normalization was done on top 3 total ion current (TIC) in addition to spectral counting.

Hierarchical clustering

The transcript clusters that were differentially expressed between ischemia and control samples, euclidean distance of expression levels was computed and hierarchical clustering performed using complete-linkage method using R Studio (3.1.1).

Gene ontology annotation

Functional categorization and pathway analysis were performed using David 6.7 Bioinformatics tool (http://david.abcc.ncifcrf.gov/) as described by (Huang et al. 2009). David Bioinformatics mainly provided batch gene annotation and Gene Ontology (GO) term enrichment analysis to highlight the most relevant GO terms associated with the uploaded gene list.

Cytoscape analysis

Differentially expressed protein *p*-values were mapped into Protein-Protein Interaction (PPI) network using Cytoscape version 3.2.1 (Shannon et al. 2003). Human PPI data were obtained from gene mania database (http://www.genemania.org/) after conversion to rat PPI using orthologous relationship ("interologs") obtained from inparanoid database (http://inparanoid.sbc.su.se/).

Brain ions determination

Whole brains were wet ashed in nitric acid (15.5 mol/L), diluted, and filtered for the determination of iron, potassium, sodium and magnesium by dual view ICP-OES.

Ultrastructure of hippocampus

Where indicated brain hippocampi were carefully dissected, immediately fixed in 3% glutaraldehyde (buffered at pH 7.4) and post-fixed in 2% osmium tetroxide. Following hydration, hippocampi were embedded in Epon 812 and ultrathin sections of the dentate gyrus area realized, stained with uranyl acetate and lead citrate and observed using a JEM 1010 transmission electron microscope.

Immunohistochemistry of hippocampus

Due to its role in memory and cognitive processes hippocampus was used for the detection of calcium burst, CD56 and CD68 inflammatory biomarkers (Eichenbaum 2004). Briefly, hippocampi were fixed in 10% (*v*/v) formaldehyde, dehydrated and embedded in paraffin. Five micrometer thick sections were stained with haematoxylin-eosin (HE) or with Von kossa reagent for calcium labeling and examined under light microscope. Sections were also deparaffinized, rehydrated and antigen retrieval realized after incubation with bond™ ready to use primary antibody against CD56 (clone CD564, catalogue number PA0191) or CD68 (clone 514H12, catalogue number PA0273) purchased from Leica Biosystems, (Newcastle upon Tyne UK) for 15 min at room temperature, followed by peroxidase conjugated secondary antibody for 8 min and revealed using diaminobenzidine (DAB) as chromogen substrate.

Statisticals

Results are expressed by mean ± SEM. Significance between groups was evaluated using Student's t test. $P < 0.05$ was considered significant. (*) indicated significance for I versus C and (§) for GI versus I.

Results

Proteomic profiling and networking

To approach the biological events occurring in the brain after transient global ischemia, a quantitative proteomic analysis of differentially expressed proteins, their ontologies and pathways in C vs I, C vs GI and I vs GI was conducted. Analysis of C vs I (pool 1) expressed proteins revealed that 108 proteins among 1614 were altered upon I/R (Table 1). Analysis of C vs GI (pool 2) identified 66 proteins among which 17 proteins were also found in pool 1. Comparison of the two pools revealed that 90 proteins from pool 1 were not modified in pool 2, thus considered as protected proteins (pool 3), and 16 proteins that were present in both pool 1 and 2 considered as unprotected proteins. Among the 49 proteins remaining in pool 2, forty were modified by GSE alone and the nine other proteins were identified when comparing C vs GI pool. Figure 1 Aillustrated the various protein pools where pool 1 and pool 3 are divided into over-expressed (enriched ontologies) and under-expressed proteins (depleted ontologies) and ontology analysis applied on each individual pool. Pool 1 and 2 have been represented in a network obtained using Gene MANIA Cytoscape plugin (version 3.3.4) that highlight the functional interactions between these proteins (Fig. 1b). Overally I/R mostly down-regulated proteins and GSE protected almost all major altered protein network.

Hierarchical clustering and heat-map

Raw data were used to draw a hierarchical clustering heat-map (Fig. 1c), delineating good reproducibility and homogeneity for the various experimental groups.

Over and under expressed proteins ontologies

108 proteins were linked to at least one annotation term within the GO biological process (BP), molecular function (MF) and cellular component (CC) categories, and identified proteins were functionally categorized based on universal GO annotation terms.

The most enriched BP was glycolysis related process. Three enriched BPs were not protected by GSE, namely complement activation, protein activation cascade and humoral immune response (Fig. 2a). Concerning under-expressed proteins (Fig. 2b), 67 terms of BPs were altered, in particular synaptic vesicle priming, followed by potassium homeostasis. Four enriched BPs were partially prevented upon GSE, among which synaptic vesicle priming.

Concerning MF ontology (Fig. 2c), 8 terms were over-represented. Metallo-amino-peptidase activity was the most abundant term representing 15% of over-expressed proteins, followed by hydro-lyase. Five MFs were not fully prevented upon GSE among which metallo-amino-peptidase and hydro-lyase activities. Analysis of under-expressed MFs showed that 26 MFs were altered among which myosin heavy chain binding (18% of under-expressed proteins) (Fig. 2d). Noticeable that ATPase activity, coupled to trans-membrane movement of ions was detected in both depleted and enhanced MFs.

Eleven terms of CC process were enriched, cytosol being the most enriched one reaching 33% (Fig. 3a). Six CCs were not fully protected by GSE among which cytosol and mitochondrion. Regarding under-expressed proteins, 34 terms were altered among which clathrin sculpted gamma-aminobutyric acid transport vesicle was the most depleted term representing 25% of under-expressed proteins (Fig. 3b) and 14 CC ontologies were partially protected by GSE.

Altered pathways and reactomes

Concerning reactomes (Fig. 3c) mitochondrial fatty acid beta-oxidation wasthe main up-regulated one followed by glycolysis, transferrin endocytosis and recycling with 25%, 13% and 13% respectively. The most depleted reactome was GABA metabolism (22%) followed by nuclear envelope reassembly (15%) (Fig. 3d).

Brain ionograme

To further support ontology data, complementary ion determinations were conducted. Free iron and sodium increased upon I/R respectively by +80% and + 100% and GSE protected them efficiently, to near control for sodium (Fig. 4a) or to lower level for free iron (Fig. 4b). On the other hand potassium (Fig. 4c) and magnesium (Fig. 4d) decreased upon I/R by 50% that were efficiently protected upon GSE.

Transmission Electron Microscopy (TEM)

Ultra-structural impairment occurring into hippocampus upon I/R was also investigated. Most nervous cells in the sham group exhibited intact and smooth nuclear membranes, well distributed chromatin and normal organelles (Fig. 5) whereas upon I/R disrupted nuclear membranes, abnormal chromatin, sparse cytoplasm and collapsed organelles were detected. Interestingly ultrastructural morphology of GI group was close to sham control.

Table 1 I/R altered proteins and GSE correction

Uniprot ID	Descrption	C	I	GI	Peptid count	Confidence score	Anova (p)	Max fold change
P49748	Very long-chain specific acyl-CoA dehydrogenase, mitochondrial	5055 ± 135,5	3477 ± 301,7	4648 ± 653,7*	25	1282,71	0,002573	3,455,258
P63267	Actin, gamma-enteric smooth muscle	3,252,000 ± 288,380	1,964,000 ± 319,599	2,179,000 ± 245,408	20	859,98	5,88E-05	7,739,726
P11137	Microtubule-associatedprotein	144,124 ± 7647	85,343 ± 8927	132,971 ± 4675*	25	1632,69	7,61E-05	2,064,409
P10809	60 kDa heat shock protein, mitochondrial	71,010 ± 8949	36,903 ± 6489	74,393 ± 4198	17	1108,72	0,005148	2,634,518
P11142	Heat shock cognate 71 kDa protein	140,279 ± 10,256	108,514 ± 7172	141,301 ± 3124*	16	1138,94	0,04833	1,262,912
Q13554	Calcium/calmodulin-dependentprotein kinase type II subunit beta	49,683 ± 11,597	19,699 ± 3189	51,614 ± 4911*	11	492,31	0,000269	894,107
Q9H4G0	Isoform L of Band 4.1-like protein 1	44,040 ± 6635	18,346 ± 1971	39,201 ± 1954*	16	862,44	8,66E-05	740,769
P50395	Rab GDP dissociation inhibitor beta	42,146 ± 8918	16,968 ± 3452	20,387 ± 917,6	4	171,56	0,000348	625,743
P61764	Syntaxin-bindingprotein 1	23,107 ± 6486	3644 ± 2236	24,217 ± 2341*	13	678,58	0,00073	2,010,513
Q00765	Reep5 protein;Receptor expression-enhancing protein 5	40,128 ± 5878	22,390 ± 3814	37,490 ± 2763*	3	238,02	0,022145	2,681,887
O75390	Citrate synthase, mitochondrial	20,474 ± 4924	4052 ± 1901	16,509 ± 1774*	8	468,1	6,45E-07	23,77,178
P61421	ATPase, H+ transporting, lysosomal 38 kDa, V0 subunit d1	33,875 ± 2001	17,479 ± 3629	26,982 ± 1318*	11	581,8	0,000278	9,744,108
O15020	Spectrin beta chain, non-erythrocytic 2	32,775 ± 6597	16,931 ± 1415	33,944 ± 3224*	9	504,09	0,000579	2,222,275
Q16623	Syntaxin-1A	37,686 ± 3897	21,870 ± 2326	37,461 ± 2467*	2	95,87	0,00041	320,579
P78356	Phosphatidylinositol 5-phosphate 4-kinase type-2 beta	39,522 ± 3849	24,024 ± 3078	37,278 ± 2971*	10	570,28	1,08E-05	3,860,319
Q9UBQ0	Vps29 protein	44,340 ± 1732	30,990 ± 3003	39,996 ± 530,0*	12	572,57	0,00334	190,339
P46821	Microtubule-associatedprotein 1B	38,145 ± 2847	27,235 ± 2127	35,894 ± 1172*	11	421,13	4,62E-05	5,026,468
Q96EQ0	Small glutamine-rich tetratricopeptide repeat-containing protein beta	18,552 ± 4024	8334 ± 779,1	17,712 ± 2581*	4	176,58	0,011948	2,808,595
P05388	60S acidic ribosomal protein P0	15,501 ± 4104	5600 ± 1034	16,780 ± 964,9*	9	542,82	0,002591	2,018,508
Q9NWU1	3-oxoacyl-[acyl-carrier-protein] synthase, mitochondrial	15,528 ± 1639	5982 ± 783,5	12,613 ± 1827*	8	365,87	0,000625	9,903,951
Q53FP2	Transmembraneprotein 35	20,319 ± 3211	11,008 ± 342,6	19,277 ± 2244*	11	620,15	0,003125	2,223,157
P17844	Probable ATP-dependent RNA helicase DDX5	18,501 ± 3490	9824 ± 843,3	16,054 ± 2657*	11	584,84	0,001087	3,391,522
P80723	Brainacid soluble protein 1	17,046 ± 2174	8839 ± 1065	8955 ± 95,41*	11	626,63	0,021677	1,729,477
Q01814	Calcium-transporting ATPase	10,989 ± 2817	4052 ± 967,5	9747 ± 789,8*	12	506,12	0,011177	248,812
P0CW22	40S ribosomal protein S17	15,075 ± 1108	8434 ± 1452	9863 ± 583,0	3	236,21	0,00241	3,655,883
P42166	Lamina-associated polypeptide 2, isoform beta	9239 ± 2083	2762 ± 968,5	8975 ± 676,0*	11	624,1	0,00511	5,043,472
P30084	Enoyl-CoA hydratase, mitochondrial	27,980 ± 2253	21,553 ± 380,9	23,088 ± 735,4*	3	222,91	8,18E-06	294,521
P26885	peptidyl-prolyl cis-transisomerase FKBP2 isoform X3	38,321 ± 1022	32,365 ± 744	38,160 ± 421,8*	10	552,59	0,042588	1,420,318
P05023	Sodium/potassium-transporting ATPase subunit alpha-1	16,871 ± 2235	10,943 ± 611,3	17,496 ± 1269*	9	402,96	0,00607	3,513,623
P00441	Superoxidedismutase [Cu-Zn]	7253 ± 874,4	1540 ± 194,2	6652 ± 1167*	9	552,8	5,80E-07	9,532,971
Q14103	RNA binding protein p45AUF1	14,219 ± 1398	8865 ± 872	13,232 ± 684,7*	8	447,84	0,000197	1,856,757
Q9P2X3	Protein IMPACT	7576 ± 1357	2342 ± 640,2	7173 ± 643,6*	8	494,76	0,027181	6,980,045
O14828	Secretory carrier-associated membrane protein 3	10,115 ± 1299	4955 ± 872,1	6013 ± 846,2	9	464,88	0,00181	2,320,972
Q9H0Q0	Protein FAM49A	12,449 ± 1010	7543 ± 1087	12,838 ± 940,0*	8	317,98	0,006062	6,720,712
O75122	CLIP-associatingprotein 2	9231 ± 1576	4413 ± 964,2	5552 ± 390,9	5	162,95	0,005476	5,859,161
Q08170	;Protein Srsf4	8050 ± 1622	3450 ± 378,8	6651 ± 347,7*	7	447,05	3,50E-06	7,143,609
P23677	Inositol-trisphosphate 3-kinase A	6980 ± 361,4	2479 ± 636,5	5848 ± 565,2*	8	599,98	0,001035	1,807,211
O75396	Vesicle-traffickingprotein SEC22b	9600 ± 818,8	5263 ± 369,8	8992 ± 840,7*	7	550,09	0,002699	21,543
Q3KRD5	Mitochondrial import receptorsubunit TOM34	10,562 ± 1525	6392 ± 455,3	10,799 ± 1035*	7	375,36	0,049136	1,627,609
Q99259	Glutamate decarboxylase 1	18,671 ± 1142	14,805 ± 344,7	18,423 ± 811,4*	6	256,13	0,002276	3,261,434
P20700	Lamin-B1	6128 ± 1422	2489 ± 513,4	5806 ± 985,4*	8	413,02	0,000589	296,066
Q00535	Cyclin-dependent-like kinase 5	7409 ± 1176	3853 ± 540,8	6505 ± 1118*	8	536,22	0,002548	2,597,922
P62750	60S ribosomal protein L23a-like	5529 ± 1245	2002 ± 337,6	2797 ± 361,2	7	301,46	0,001858	2,264,326
P31323	cAMP-dependent protein kinase type II-beta regulatory subunit	7515 ± 755,6	4097 ± 193,2	6561 ± 499,4*	7	349,74	0,001509	7,479,962
Q14289	Protein-tyrosine kinase 2-beta	6412 ± 1091	2995 ± 351,3	5541 ± 634,9*	8	361,78	6,90E-05	2,690,438
P04843	Dolichyl-diphosphooligosaccharide--proteinglycosyltransferasesubunit 1	4894 ± 1057	1693 ± 366,6	4129 ± 269,1*	3	142,35	5,08E-06	23,94,797
Q16799	Reticulon-1	4796 ± 585,0	1605 ± 436,6	4256 ± 395,0*	5	253,8	0,001059	7,122,095

Table 1 (continued)

Uniprot ID	Descrption	C	I	GI	Peptid count	Confidence score	Anova (p)	Max fold change
P08133	Annexin A6	7177 ± 819,5	4151 ± 551,5	5767 ± 970,1*	7	460,83	0,004801	2,584,196
Q13557	Calcium/calmodulin-dependentprotein kinase type II subunit delta	9157 ± 128,0	6202 ± 810,1	8739 ± 252,7*	7	297,33	0,000219	21,91,005
P51648	Fattyaldehydedehydrogenase	4272 ± 915,1	1494 ± 352,4	2017 ± 232,5	7	300,18	0,018354	1,733,637
Q16352	Alpha-internexin	3115 ± 52,39	430,6 ± 168,4	3523 ± 277,5*	2	64,68	0,00036	20,40,332
Q16653	myelin/oligodendrocyte glycoprotein;	2726 ± 1471	197,4 ± 12,66	2315 ± 181,4*	7	393,43	2,30E-06	22,35,441
P06576	ATP synthase subunit beta, mitochondrial	2949 ± 904,4	567,0 ± 142,8	2264 ± 592,6*	4	182,12	0,000556	17,66,827
P49368	T-complexprotein 1 subunit gamma	3781 ± 384,4	1415 ± 359,9	1787 ± 398,0	4	289,71	0,019728	238,443
Q9Y6E0	Serine/threonine-protein kinase 24	3843 ± 547,4	1758 ± 415,7	3206 ± 187,6*	4	257,68	0,012597	2,091,177
O60641	Clathrincoatassemblyprotein AP180	4241 ± 516,3	2211 ± 398,3	3846 ± 638,3*	8	373,97	0,00102	3,012,692
Q9NQX3	Gephyrin	2507 ± 592,4	497,0 ± 68,12	2217 ± 117,8*	5	224,58	0,003377	328,009
P25786	Proteasomesubunit alpha type-1	3205 ± 313,8	1586 ± 289,9	1893 ± 136,9	6	405,87	0,043391	2,600,922
Q15700	Disks large homolog 2	3393 ± 106,5	1903 ± 317,5	2606 ± 905*	5	215,98	0,007634	2,588,708
O94925	Glutaminase kidney isoform, mitochondrial	2491 ± 556,1	1004 ± 120,1	2210 ± 216,6*	7	438,47	0,019917	2,255,259
Q96EY1	Tid-1 long isoform	1570 ± 448	238,8 ± 153,9	1431 ± 140,4*	7	353,45	0,007204	2,106,677
Q8IYB5	Stromal membrane-associatedprotein 1	2541 ± 405,7	1314 ± 197,7	1304 ± 142,8	6	340,61	0,001606	2,112,866
Q96SB3	Neurabin-2	1258 ± 203,5	178,2 ± 85,22	1105 ± 199,5*	7	327,8	0,008212	2,630,158
Q9Y2J0	Rabphilin-3A	2863 ± 347,7	1864 ± 109,9	2294 ± 454,9*	5	178,82	0,002048	207,256
P28289	Tropomodulin 1	2437 ± 62,33	1531 ± 138,8	1702 ± 147,9	6	305,04	1,51E-05	2,521,176
O00330	Pyruvate dehydrogenaseprotein X component, mitochondrial	1736 ± 209,2	830,7 ± 162,4	1389 ± 45,23*	3	91,77	1,66E-05	801,897
Q00610	Clathrinheavychain 1	2714 ± 209,2	2030 ± 133,8	1790 ± 943	6	424,11	0,015616	1,923,146
O95674	Phosphatidatecytidylyltransferase 2	1141 ± 179	468,6 ± 123	1076 ± 75,26*	6	305,39	0,006727	23,223
P13521	Secretogranin-2	1458 ± 165,5	951,7 ± 91,29	1437 ± 205,7*	5	189,42	1,32E-05	14,36,003
P62807	Histone H2B type 1	858,9 ± 73,81	441,5 ± 91,81	864,0 ± 36,90*	4	247,7	0,000961	2,632,955
P16949	Stathmin	381,3 ± 156,7	65,16 ± 20,45	275,1 ± 40,06*	4	192,1	0,001819	2,216,247
Q99962	Endophilin-A1	277,7 ± 90,7	39,82 ± 15,85	263,7 ± 34,49*	2	80,88	0,025369	1,426,053
P31146	Coronin-1A	201,2 ± 41,54	78,22 ± 15,81	166,7 ± 20,71*	5	371,58	3,27E-07	4,728,283
Q07021	Complement component 1 Q subcomponent-bindingprotein, mitochondrial	31,28 ± 9018	124,9 ± 2905	43,99 ± 6811*	3	142,25	0,019028	3,848,112
Q92499	ATP-dependent RNA helicase DDX1	1040 ± 0,5626	223,6 ± 99,64	5504 ± 3677	5	224,93	0,000107	2,980,979
Q99798	Aconitate hydratase, mitochondrial	0,0 ± 0	415,5 ± 235,8	1973 ± 0,9180	6	216,04	0,004936	3,158,173
P16615	Sarcoplasmic/endoplasmic reticulum calcium ATPase 2	700,3 ± 53,88	1117 ± 54,05	766,1 ± 74,16*	5	184,64	0,000154	2,290,602
Q99623	Prohibitin-2	2356 ± 2356	493,4 ± 96,53	20,62 ± 1349	5	209,17	0,002807	1,645,111
P11217	Alpha-1,4 glucanphosphorylase	2186 ± 124,9	2816 ± 67,77	2407 ± 146,1*	5	224	0,001864	2,422,725
O43301	Heat shock 70 kDa protein 12A	166,4 ± 34,78	873,7 ± 256,9	485,1 ± 167,9	5	305,1	0,000116	4,790,286
P61353	60S ribosomal protein L27	106,0 ± 24,12	806,4 ± 118,6	284,8 ± 62,97	5	230,07	0,003263	2,566,074
Q93077	Histone H2A type 4	352,8 ± 133,2	1398 ± 82,77	417,5 ± 103,1*	4	194,95	0,000588	2,906,151
Q16401	Proteasome	625,7 ± 76,65	1690 ± 273,2	820,0 ± 74,46*	4	184,59	0,000198	2,457,571
Q01813	ATP-dependent 6-phosphofructokinase, platelet type	0,9254 ± 0,9162	1134 ± 684,5	1266 ± 1154*	4	209,63	0,008342	2,664,819
Q189C4	Glyceraldehyde-3-phosphate dehydrogenase	150,35 ± 3,51	1209,471 ± 12,95	196,301 ± 5963	9	490,67	0,000275	8,044,369
P55786	ProteinNpepps	520,8 ± 172,1	1694 ± 423,2	1334 ± 235,5	5	213,02	0,001094	2,481,745
P49720	Proteasomesubunit beta type-3	986,7 ± 308,1	2232 ± 185,2	1223 ± 264,7*	5	207,95	0,000118	10,09238
P14324	Farnesyl pyrophosphate synthase	1490 ± 409,7	3826 ± 230	1852 ± 348,8*	4	257,75	0,002218	2,481,753
P17987	T-complexprotein 1 subunit alpha	1316 ± 285,8	3668 ± 208,9	1663 ± 215,6*	5	282,22	0,000185	2,233,257
Q9UHG2	ProSAAS	5842 ± 616,2	8212 ± 205,9	8866 ± 685,1	3	124,17	0,004416	3,441,157
P49591	Serine--tRNA ligase, cytoplasmic	4014 ± 489,8	6496 ± 631	5488 ± 312,6*	4	119,72	0,001994	6,215,821
P19338	Nucleolin	2988 ± 72,94	5989 ± 1157	3523 ± 246,9*	3	163,85	0,015476	23,59,006
P16152	Carbonylreductase [NADPH] 1	2951 ± 417,1	6271 ± 932,5	3550 ± 316,6*	5	221,5	0,000344	20,9491

Table 1 (continued)

Uniprot ID	Descrption	C	I	GI	Peptid count	Confidence score	Anova (p)	Max fold change
Q9NQW7	Xaa-Pro aminopeptidase 1	2642 ± 583,3	7031 ± 1275	3715 ± 483,2*	5	223,26	0,001196	5,184,988
P02787	Serotransferrin	1575 ± 325,9	6314 ± 2143	2301 ± 167,9*	3	86	0,008526	1,976,915
P48539	Purkinje cellprotein 4	733,5 ± 71,19	5462 ± 2418	1073 ± 278,3*	4	259,5	0,005952	2,926,054
P52943	Cysteine-richprotein 2	9333 ± 1252	15,045 ± 1255	19,861 ± 635,9	4	162,61	6,47E-05	2,780,319
O95716	GTP-binding protein Rab-3D	14,836 ± 1233	22,478 ± 1308	11,216 ± 217,5*	4	179,22	1,10E-08	6,255,352
P35520	Cystathionine beta-synthase	8688 ± 851,8	16,892 ± 881,7	35,791 ± 2523*	4	222,81	0,011336	3,460,626
P09104	Gamma-enolase	21,278 ± 756,2	39,152 ± 1327	23,695 ± 1787*	7	492,69	0,000268	1,840,022
P09488	Glutathione S-transferase Mu 1	32,357 ± 2207	40,822 ± 1028	34,611 ± 838,9*	2	157,22	0,002264	2,183,475
P38606	V-type proton ATPase catalyticsubunit A	3350 ± 764,3	12,190 ± 3580	24,433 ± 1311	4	189,09	0,027441	2,326,795
P23528	Cofilin 1	18,137 ± 426,8	29,380 ± 2371	41,019 ± 632,4*	4	356,45	4,28E-09	7,832,123
P14618	Pyruvate kinase PKM	32,932 ± 3669	65,290 ± 5709	23,345 ± 9445*	4	290,36	0,01145	1,435,242
Q14195	Dihydropyrimidinase-relatedprotein 3	223,320 ± 7724	258,271 ± 8152	54,132 ± 3033*	4	207,46	0,011266	299,785
P06733	Alpha-enolase	46,996 ± 1393	94,202 ± 18,701	79,975 ± 5318*	37	1894,56	0,000179	2,816,599
P09972	Fructose-bisphosphatealdolase C	71,595 ± 9159	141,174 ± 3072	262,869 ± 21054*	25	1282,71	0,002573	3,455,258
P69905	Hemoglobinsubunit alpha-1/2	241,230 ± 15,774	360,367 ± 35,946	995,859 ± 94381*	20	859,98	5,88E-05	7,739,726

Immunohistochemistry analysis

Immuno-detection of CD56 and CD68 biomarkers, used to evaluate inflammation that occurred into stressed hippocampus, supported data of proteomic analysis in such a way that I/R decreased CD56 (also called NCAM) but increased CD68 labeling and GSE protected these disturbances till control level (Fig. 6, Fig. 7).Von kossa staining evidenced the I/R-induced calcium burst as well as the prevention afforded by GSE (Fig. 8).

Discussion

The present work investigated the proteomic changes occurring after brain I/R injury as well as the putative prevention afforded by GSE pre-treatment. Oxygen and glucose deprivation (OGD) occurring after altered blood supply leads to ATP depletion within few minutes (Caplan 2000), inducing the inactivation of Na^+/K^+ and Ca^{2+} ATPases (Racay et al. 1998), alteration of neurons and glial cells membrane potential, opening of voltage-dependent Ca^{2+} and Na^+ channels, giving rise to the first wave of excitotoxicity and cell death (Yamashita 2012). The burst in calcium constitutes one of the most critical events triggering proteases activities as calpain (Kadri et al. 2015) or phospholipase A2 and protein kinases (Won et al. 2002; Kadri et al. 2015) leading *in fine* to cell death.

The abundance of 108 proteins was altered upon I/R which is quite high when compared to previous studies (Zhang et al. 2011; Chen et al. 2015). The use of global transient model of brain ischemia and early reperfusion allows the standardization of the whole brain behavior to I/R insult, which might explain why proteomic studies of focal ischemia always reveal a limited number of altered proteins.

Over-expressed proteins ontology reveals that most enriched BPs are related to glycolysis process. Depletion of ATP and lack of cellular energy force the brain towards urgent energy fueling via anaerobic glycolysis and similar data were described for OGD cultured astrocytes (Amaral et al. 2010). Moreover, NADH and NADPH metabolic processes are upregulated upon I/R. NAD metabolism is a key process in brain function and NAD/NADH ratio a good indicator of brain energy disposal. Previous studies reported the imbalance of NAD/NADH ratio upon ischemia (Ma et al. 2015) and NADPH has even been proposed as a drug candidate in the treatment of ischemic stroke (Li et al. 2016).

Iron related processes are also enriched BPs as confirmed by high free iron level upon I/R (data not shown) and in accordance with our previous work on I/R-induced transition metal disturbances constituting one of the earliest events at the basis of the ischemic insult (Kadri et al. 2015). Mechanisms underlying iron accumulation into the brain are still unresolved but a

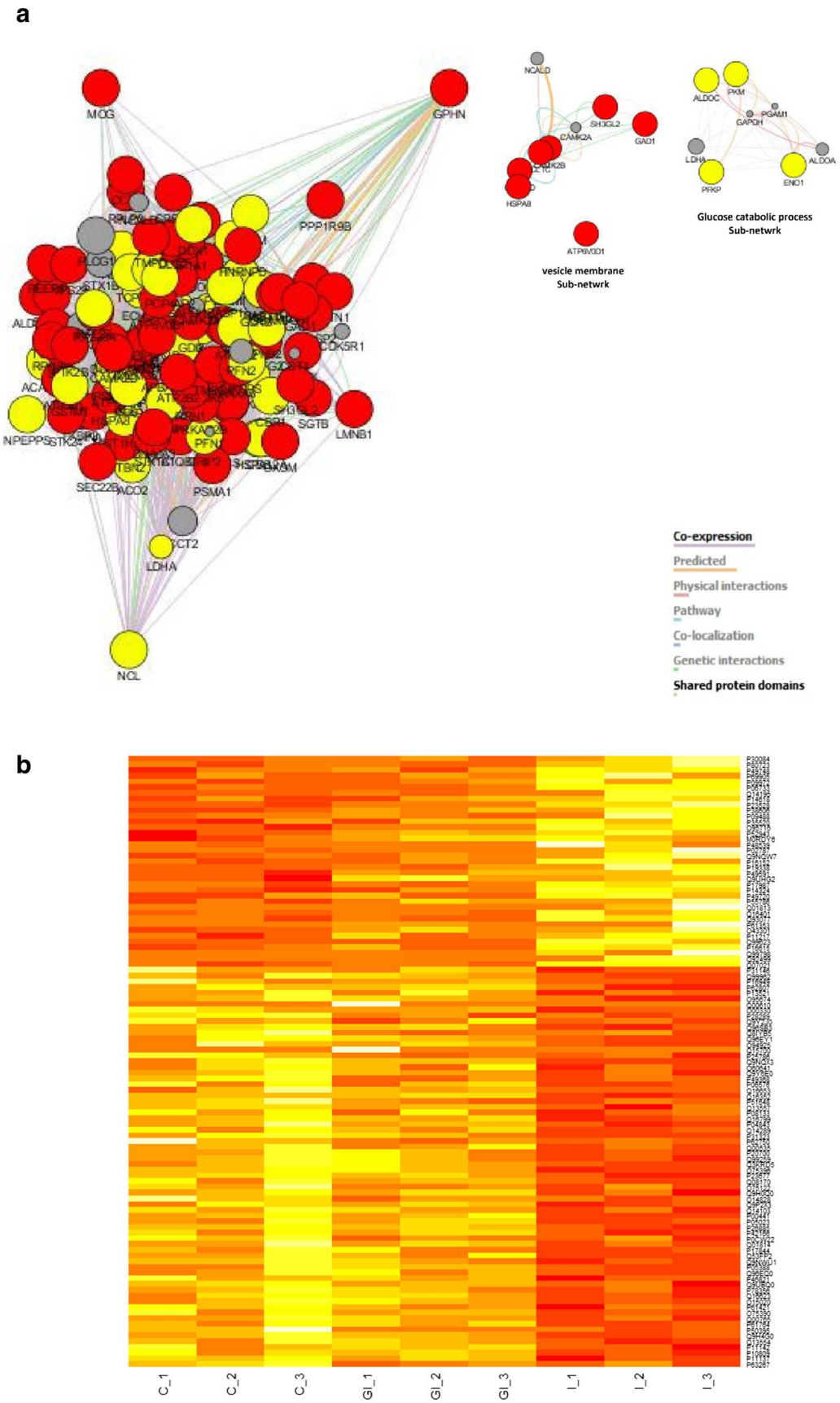

Fig. 1 **a** Cytoscape network. Proteomic data were mapped on protein-protein interaction network. Red color indicates under-expressed proteins and yellow color over-expressed proteins. **b** Hierarchical clustering of differentially expressed proteins (C = Control; I = I/R; GI = GSE + I/R)

putative way could be the rapid burst of free iron through L-type calcium channels (Oudit et al. 2006). However we have no idea on the mechanism of I/R-induced depletion of other transition metals as Cu, Zn or Mn. Noticeably is the depletion in Cu/Zn SOD abundance confirming the decrease in Cu/Zn isoform activity (Kadri et al. 2015) or of glutaminase abundance, a Mn dependent enzyme.

Under-expressed proteins are also involved in several BPs and the synaptic vesicle priming process the most down regulated BP. Other BPs related to synaptic function such as synaptic vesicle fusion to pre-synaptic membrane or synaptic vesicle endocytosis are also down regulated, likely altering most synaptic contacts. Our data are in line with those of (Fernandes et al. 2014) who showed that ischemia triggers a transcriptional response to down-regulate synaptic proteins and that inhibition of synaptic functioning is considered protective to ensure minimal brain injury.

Most enhanced MFs are peptidase and lyase activities, leading to the first wave of cell death within the ischemic core as described for calpain (Curcio et al. 2016). Enhancement of protease activity may also be associated with the switch to alternative energy fueling i-e from glycolysis to lipolysis. Although calpain activation is considered as one of the earliest events of stroke (Jiang et al. 2004), its delayed and sustained activity may play a great role in the development of ischemia-induced dementia.

Myosin heavy chain binding constitutes one of the most depleted MFs, followed by neurotransmitter vesicle docking and priming which are related to neurofilament disorganization and degradation. (Schafer et al. 2009) argued for the implication of calpain in the degradation of ankyrin G and beta IV spectrin. Modulation of such MFs in the brain could also explain the biological remodeling leading to the alteration in exocytosis process.

Concerning proteins localization, under-expressed and over-expressed proteins are clearly not distributed uniformly in the various cellular compartments. Major under-expressed proteins are located in the prolongations more exactly in the clathrin-sculpted vesicle, as I/R dropped the proteins associated to vesicle endocytosis and recycling. One putative explanation could be the calpain-induced hydrolysis of α and $\beta_2$adaptins leading to a fall in clathrin-dependent endocytosis (Rudinskiy et al. 2009). Noticeably that under-expressed proteins are also located at the dendritic shaft and spine, neuron spine and main axon, suggesting the down-regulation of synaptic activity and plasticity upon I/R whereas most over-expressed proteins are located at the cytosol and cell body. Moreover, non-membrane bound organelles such as ribosome, proteasome and microtubule organizing center are also enhanced upon I/R which confirm previous data (Caldeira et al. 2014). Proteasome related proteins (26S proteasome), non-ATPase regulatory subunit 5 (PSMD5) and proteasome subunit beta type-3 are over-expressed as well

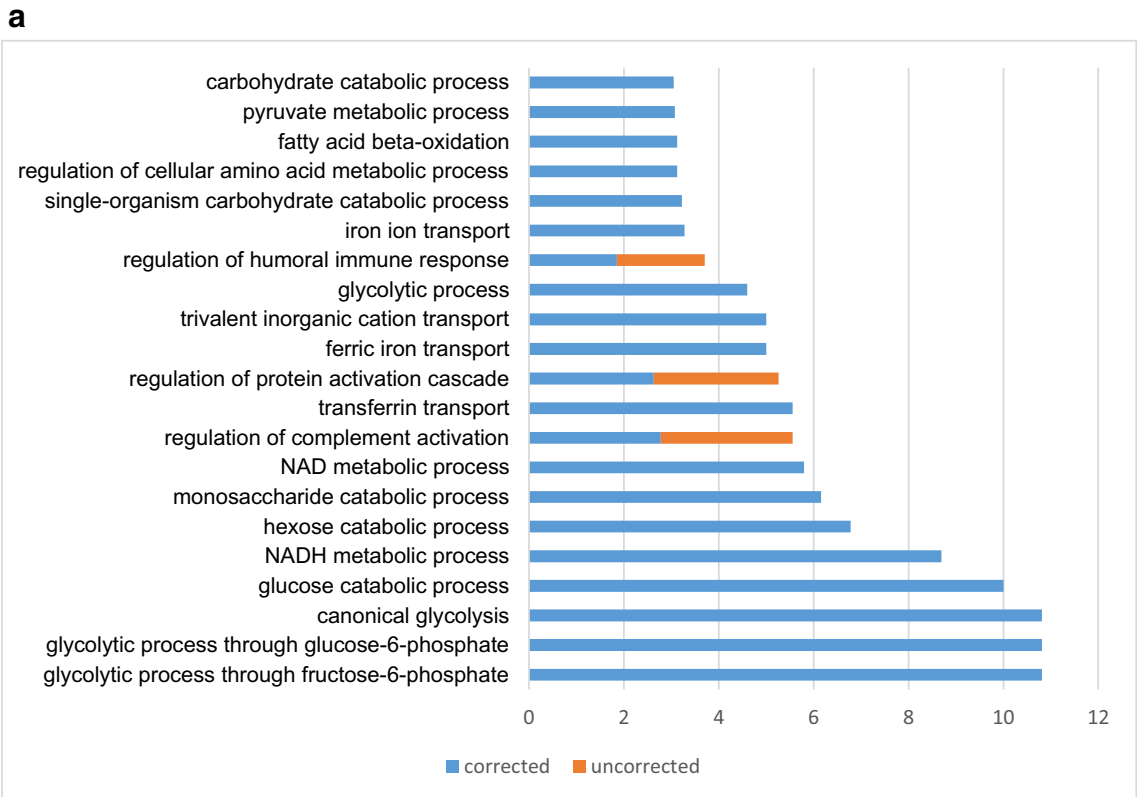

Fig. 2 Up (**a**) and down-regulated BP (**b**) and Up (**c**) and down-regulated MF (**d**) upon I/R insult and GSE correction

b

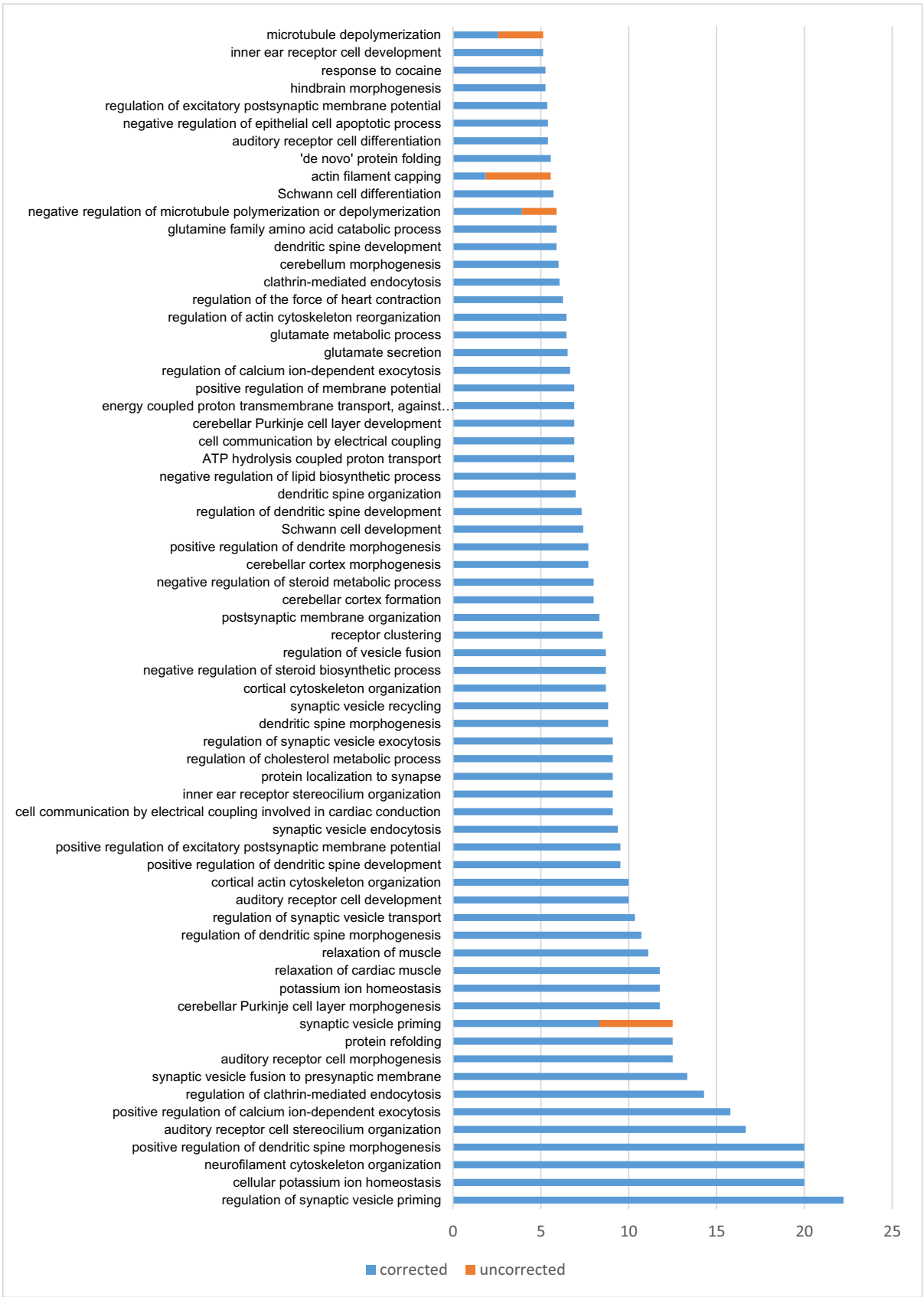

Fig. 2 (continued)

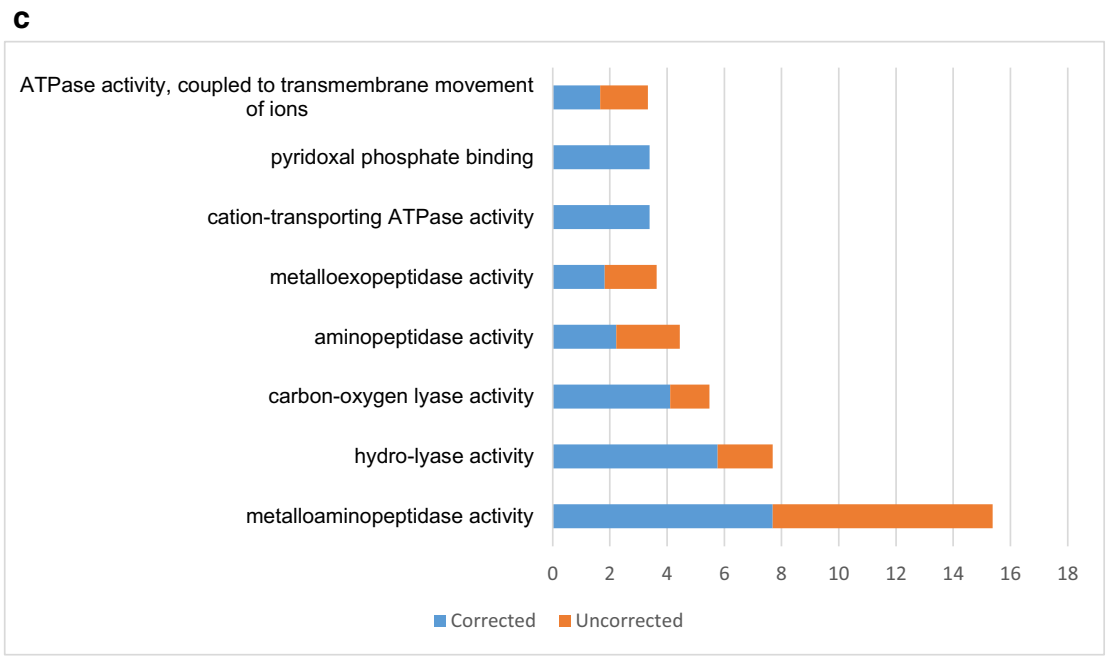

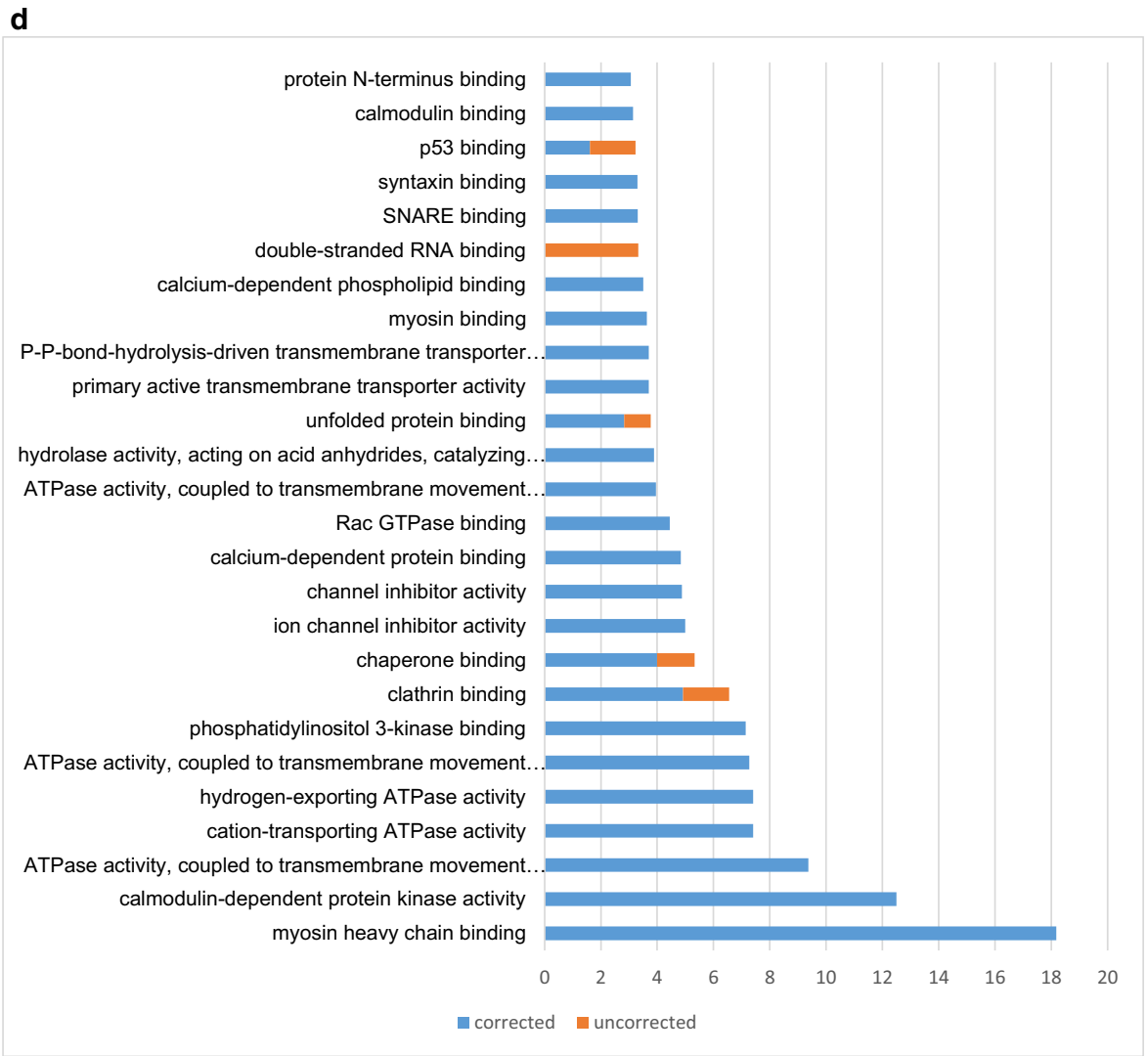

Fig. 2 (continued)

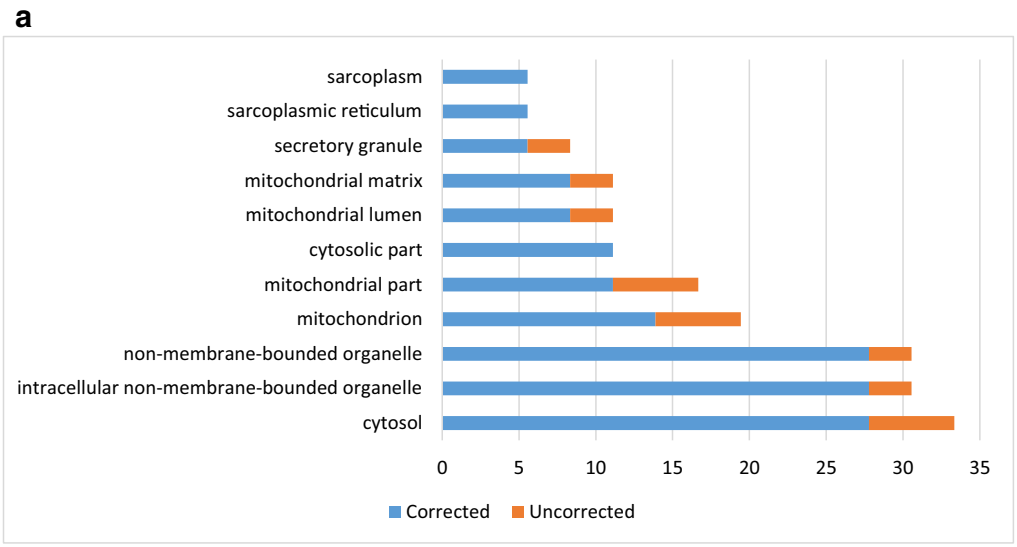

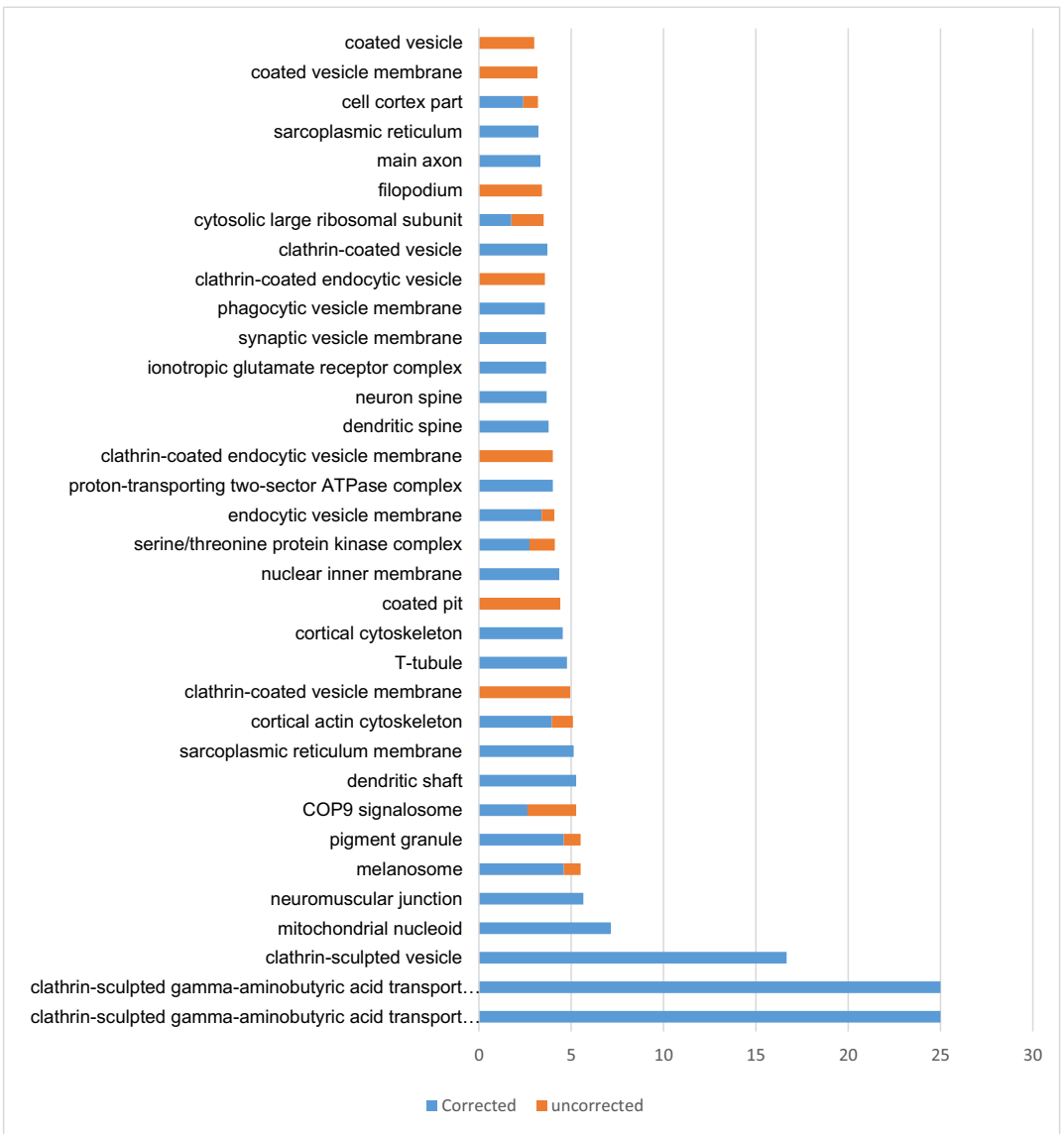

Fig. 3 Up (**a**) and down-regulated CC (**b**) and Up (**c**) and down-regulated reactomes (**d**) upon I/R insult and GSE correction

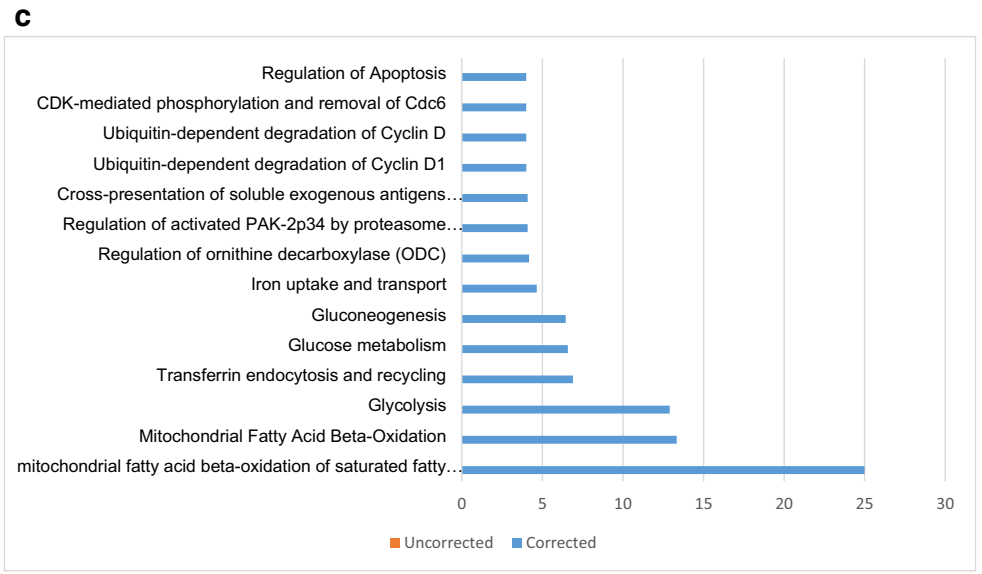

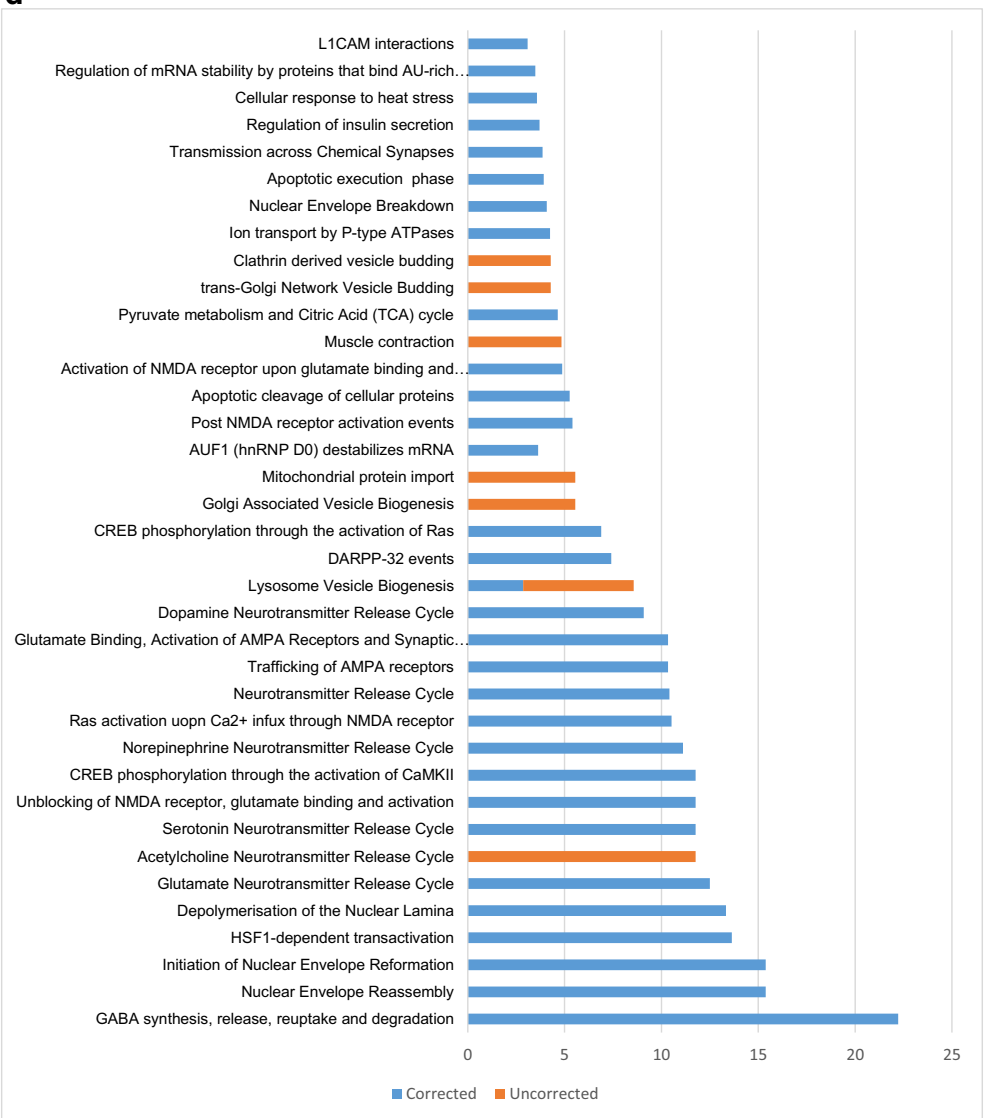

Fig. 3 (continued)

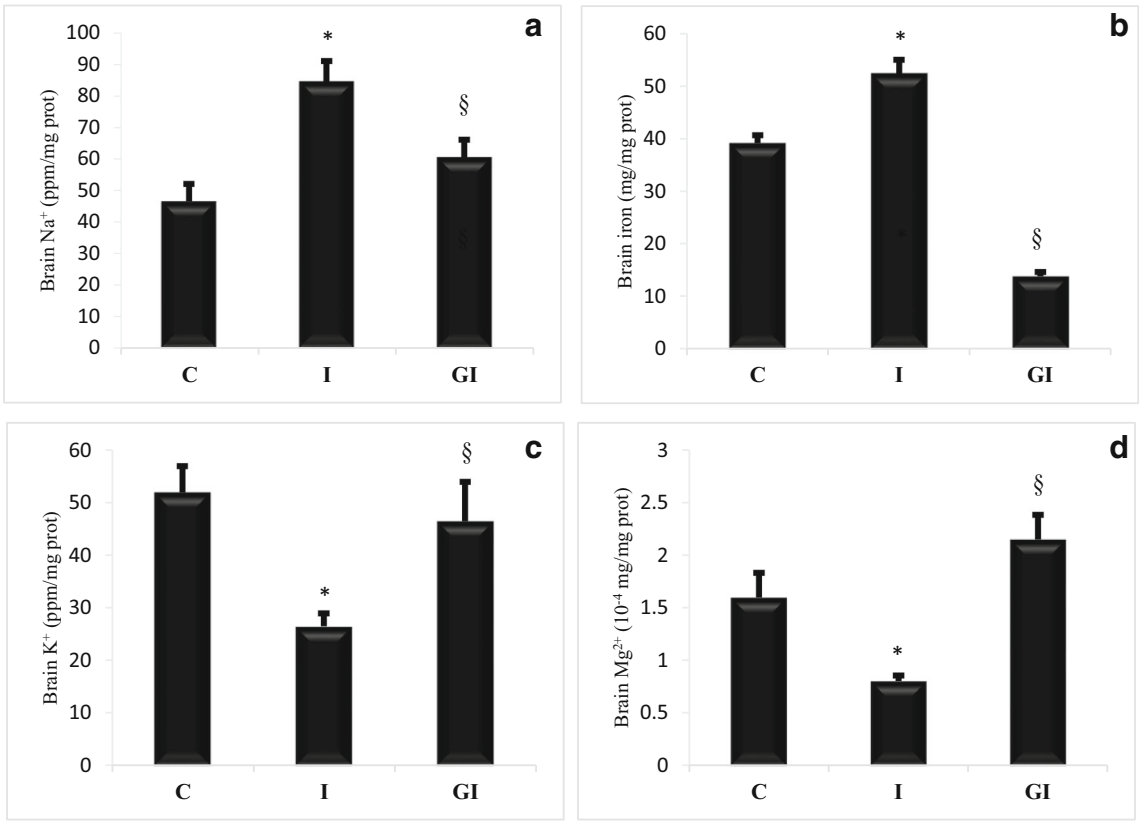

Fig. 4 Effect of I/R and GSE on brain sodium (**a**), labile iron (**b**), potassium (**c**), and magnesium (**d**)

andPSMD5 was proven to be implicated in 26S proteasome assembly and activity (Shim et al. 2012).

I/R provokes plentiful physiological changes in the brain as assessed by reactome enrichment analysis. Ischemia enhances mitochondrial fatty acid beta-oxidation which could represent an alternative pathway for cell fueling. Such data were previously described by (Ma et al. 2010) who found that fatty acid-binding proteins 5 and 7 expression increased after ischemic brain damage in a primate model. Along with fatty acid beta-oxidation, glycolysis and related reactomes as gluconeogenesis are also enhanced and these data fully support the BP ontology enrichment. It is also important to underline that I/R induces the down-regulation of almost all neurotransmitter release cycle such as glutamate, acetylcholine, serotonin, norepinephrine, dopamine and that such effects are likely linked to energy depletion (Boulland and Levy 2005).

GABA metabolism is one of the most depleted reactome and GABA the major inhibitory neurotransmitter and modulator of excitability, implicated in the reduction of glutamate release. Recent studies showed that OGD decreased GABA receptor recycling and expression thus contributing to neuronal death (Mele et al. 2016). Furthermore I/R decreasing the nuclear envelope reassembly reactome is fully supported by our current ultrastructural observation of the nuclear membrane disappearance in cells of the dentate gyrus area and also by previous related studies (Zhang et al. 2015).

Almost all disturbances on protein abundance generated upon ischemia are prevented by GSE pretreatment reaching78% of altered proteins. GSE prevents from major changes in BP enhancement except partial enrichment of some terms associated with inflammation such as complement activation and humoral immune response.

GSE corrects several key glycolytic enzymes as GAPDH, enolase, pyruvate kinase and aldolase that are up-regulated upon I/R. GAPDH was implicated in ATP synthesis at the synaptic terminal(Ikemoto et al. 2003) and played a critical role in cell death after glutamate-induced neuronal excitotoxicity inducing apoptotic cell death by means of its nuclear translocation and complexation with P_{53} (Zhai et al. 2014) or with PARP-1 (Nakajima et al. 2015). GAPDH has even been assimilated to a GABA receptor kinase that links glycolysis to neurotransmission (Laschet et al. 2004) and several reports highlighted its involvement in neuro-degeneration by means of non-glycolytic activity as protein oligomerization (Qvit et al. 2016) as occuring in the brain of AD patients (El Kadmiri et al. 2014). Although GAPDH increase is not strictly linked to reperfusion, this latter enhanced GAPDH overexpression (Tanaka et al. 2002). Accordingly GAPDH activity is clearly enhanced upon I/R and restored to near control in the presence of GSE (data not shown). Enolase exhibited important functions for brain cell survival as protection from amyloidβ accumulation and glutamate excitotoxicity

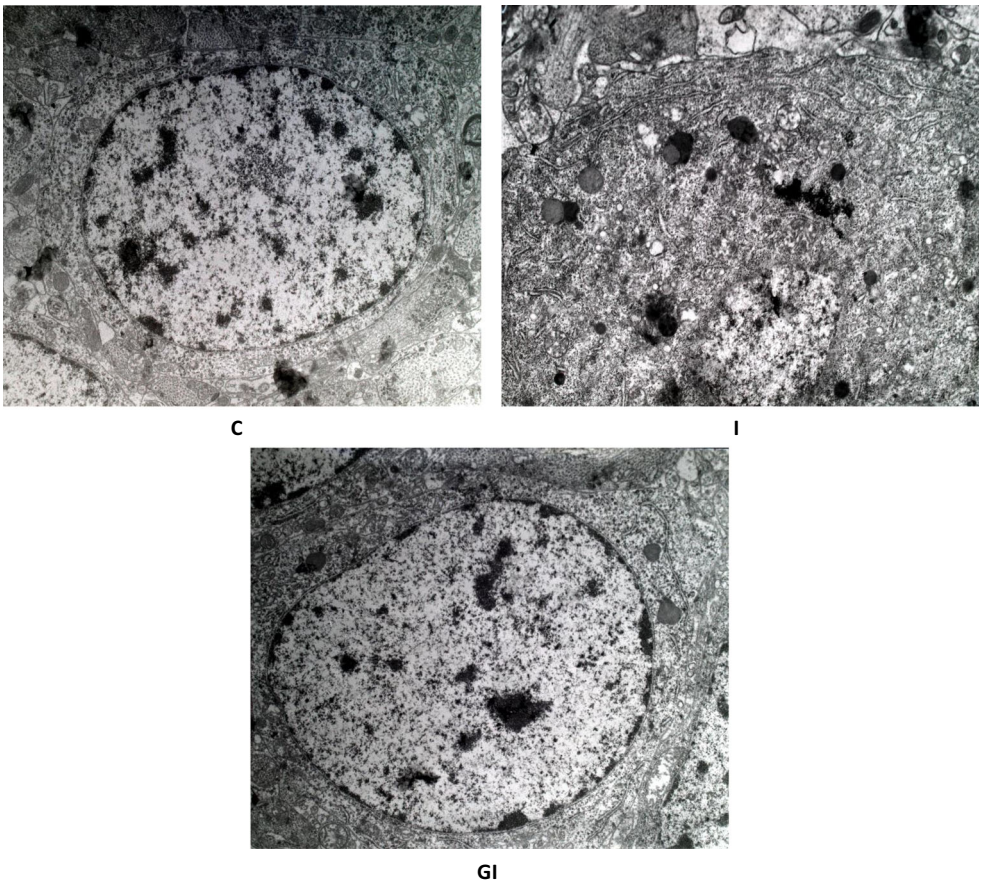

Fig. 5 Effect of I/R and GSE on hippocampal dentate gyrus area ultrastructure. Sham group exhibited intact and smooth nuclear membranes, well distributed chromatin and normal organelles although ischemia (I) group exhibited disrupted nuclear membranes, abnormal chromatin, sparse cytoplasm and collapsed organelles, whereas GSE treated animals exhibited ultrastructural appearance (GI) close to control

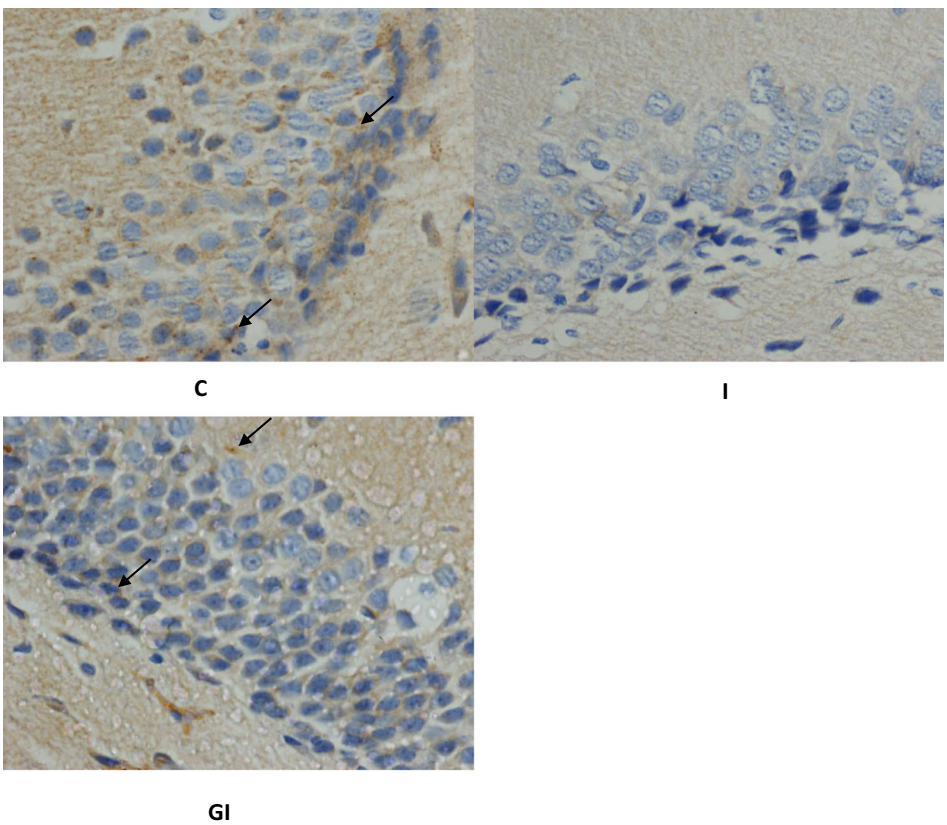

Fig. 6 Immunohistochemistry of CD56 antigen into dentate gyrus area (arrows: brown color). CD56 labeling decreasing upon I/R (I) and restored with GSE (GI) till control level (C)

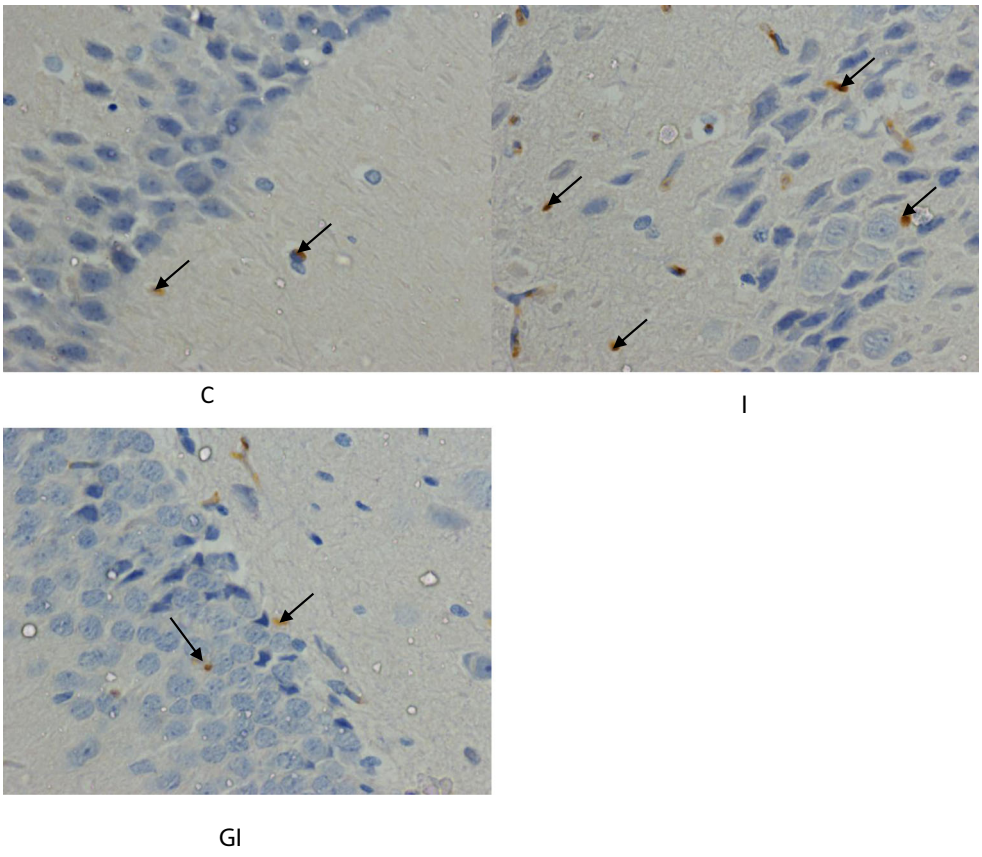

Fig. 7 Immunohistochemistry of CD68 antigen into dentate gyrus area (arrows: brown color). CD68 staining increasing upon I/R (I) and restored with GSE (GI) to near control level (C)

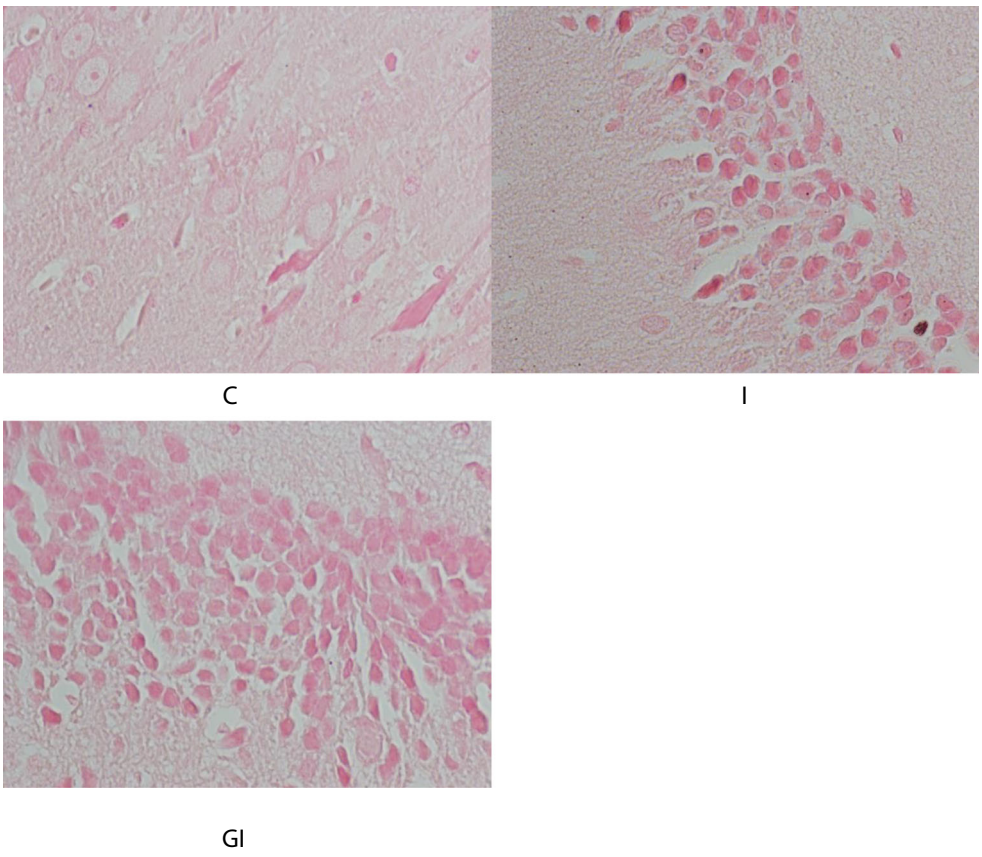

Fig. 8 Von kossa staining of calcium into dentate gyrus area (pink color). Calcium burst occurring upon I/R(I) was restored with GSE(GI) to near control level(C)

(Butterfield and Lange 2009) and aldolase, another key glycolytic enzyme, was recently reported to be strongly enhanced (5 fold) in the ischemic cortex (Chen et al. 2014). Overally, it seems that brain cells especially astrocytes, respond to hypoxia by increasing glycolytic pathway, to cope with OGD insult for providing sufficient ATP for cell survival (Marrif and Juurlink 1999). Nonetheless glycolytic enzymes functioning as moonlighting proteins should also be considered (Gancedo et al. 2016).

Likewise, GSE prevents the depletion of synaptic vesicle priming, ion homeostasis and many other terms. Thus for instance GSE protects from I/R-induced magnesium, potassium and sodium dyshomeostasis likely by acting on key protein abundances or post translational alterations as ion transporting ATPases. In this respect $Mg^{2+}$was recently shown to protect against the bio-energetic consequences as cellular ATP breakdown that occurs after glutamate excitotoxicity (Clerc et al. 2013). Furthermore GSE potently restores the abundance of the microtubule associated 1 β protein, spectrin β chain, SNARE protein Sec22b, α internexin, neurabin2, rabphilin-3A, the synaptic vesicle calcium dependent protein stathmin, the synaptic vesicle endocytosis protein endophilin A1 and coronin1A, an actin binding protein. GSE partially corrects other cytoskeleton proteins such as γ actin, CLIP associating protein2, tropomodulin1, but not clathrin dependent endocytosis as stromal membrane associated protein or clathrin heavy chain1and cofilin1. In addition we also identify other GSE-protected proteins such as secretory factor like secretogranin II, Purkinje cell protein 4 (PEP19), Pro-SAAS and dihydropyrimidinase-like 3 (Dpysl3). In fact, secretogranin II coupled to enolase and through its derived neuropeptide secretoneurin, are known to act directly on neurons after ischemic insult allowing their survival by activating theJak2/Stat3 pathway(Shyu et al. 2008). PEP19 is also neuroprotective via its implication in calmodulin inhibition following glutamate excitotoxicity as well as Pro-SAAS through the inhibition of Aβ1–42induced cytotoxicity (Hoshino et al. 2014) and Dpysl3, a member of the collapsin response mediator protein family, implicated in the inflammatory reaction of microglia through inhibition of the phagocytosis process (Manivannan et al. 2013). By acting simultaneously on this large array of proteins, GSE appeared as a multifaceted and multi-targeted mixture capable of efficient neuroprotection via its well established antioxidant and anti-inflammatory properties (Mezni et al. 2017b) which confirmed recent proteomic data on GSE efficiency against lithium neurotoxicity (Mezni et al. 2017a).

The use of high dosage GSE (2,5 g/kg) is a highly relevant feature which was inspired from the pionneering work of (Bagchi et al. 2000) and other subsequent studies that led to the elaboration of calibrated commercial preparations of GSE (Li et al. 2015). Owing to its safety and tolerability, GSE is increasingly used at high dosage (1-4 g/kg) according to our own data (Mokni et al. 2012; Charradi et al. 2013; Kadri et al. 2015; Khazri et al. 2016) or to current literature (Li et al. 2015; Margalef et al. 2015) as we recently demonstrated the lack of any toxicity and the dose effect safety till high dosing range GSE reaching the tremendous dosage of 16 g/kg (Charradi et al. 2018). In addition repeated high dosing range GSE improving polyphenols bioavailability into the brain (Charradi et al. 2018), the translational application of high dosage GSE in the prevention of human stroke is realistic as we already conducted clinical trials on chronic kidney disease patients administered with repeated high dosing GSE with no side effects nor drop out during the 6 month-long treatment (Turki et al. 2016).

Conclusion

This work provides evidence of the potent prevention of GSE on brain ischemia, paving the way to clinical trials targeting high risk or predisposed stroke patients that should be undertaken rapidly due to the safety and tolerability of high dosage and GRAS certified GSE.

Acknowledgments Mr. Ridha Charada, head of the Cave Neferis is gratefully acknowledged for providing grape pomace and Mrs. Awatef Ben Ammar for performing TEM imaging.

Compliance with ethical standards

Conflict of interest None.

References

Amaral AI, Teixeira AP, Martens S et al (2010) Metabolic alterations induced by ischemia in primary cultures of astrocytes: merging 13C NMR spectroscopy and metabolic flux analysis. J Neurochem 113:735–748. https://doi.org/10.1111/j.1471-4159.2010.06636.x

Bagchi D, Bagchi M, Stohs SJ et al (2000) Free radicals and grape seed proanthocyanidin extract: importance in human health and disease prevention. Toxicology 148:187–197

Boulland J-L, Levy LM (2005) Glutamate, glutamine and ischaemia in the central nervous system. Tidsskr Nor Laegeforen 125:1479–1481

Butterfield DA, Lange MLB (2009) Multifunctional roles of enolase in Alzheimer's disease brain: beyond altered glucose metabolism. J Neurochem 111:915–933. https://doi.org/10.1111/j.1471-4159.2009.06397.x

Caldeira MV, Salazar IL, Curcio M et al (2014) Role of the ubiquitin-proteasome system in brain ischemia: friend or foe? Prog Neurobiol 112:50–69. https://doi.org/10.1016/j.pneurobio.2013.10.003

Caplan LR (2000) Caplan's stroke: a clinical approach. Butterworth-Heinemann

Chao C-L, Chang N-C, Weng C-S et al (2011) Grape seed extract ameliorates tumor necrosis factor-α-induced inflammatory status of

human umbilical vein endothelial cells. Eur J Nutr 50:401–409. https://doi.org/10.1007/s00394-010-0151-6

Charradi K, Elkahoui S, Karkouch I et al (2012) Grape seed and skin extract prevents high-fat diet-induced brain lipotoxicity in rat. Neurochem Res 37:2004–2013. https://doi.org/10.1007/s11064-012-0821-2

Charradi K, Mahmoudi M, Elkahoui S et al (2013) Grape seed and skin extract mitigates heart and liver oxidative damage induced by a high-fat diet in the rat: gender dependency. Can J Physiol Pharmacol 91:1076–1085. https://doi.org/10.1139/cjpp-2013-0225

Charradi K, Mahmoudi M, Bedhiafi T et al (2018) Safety evaluation, anti-oxidative and anti-inflammatory effects of subchronically dietary supplemented high dosing grape seed powder (GSP) to healthy rat. Biomed Pharmacother Biomedecine Pharmacother 107:534–546. https://doi.org/10.1016/j.biopha.2018.08.031

Chen Y-H, Chiang Y-H, Ma H-I (2014) Analysis of spatial and temporal protein expression in the cerebral cortex after ischemia-reperfusion injury. J Clin Neurol 10:84–93. https://doi.org/10.3988/jcn.2014.10.2.84

Chen J-H, Kuo H-C, Lee K-F, Tsai T-H (2015) Global proteomic analysis of brain tissues in transient ischemia brain damage in rats. Int J Mol Sci 16:11873–11891. https://doi.org/10.3390/ijms160611873

Clerc P, Young CA, Bordt EA et al (2013) Magnesium sulfate protects against the bioenergetic consequences of chronic glutamate receptor stimulation. PLoS One 8:e79982. https://doi.org/10.1371/journal.pone.0079982

Curcio M, Salazar IL, Mele M et al (2016) Calpains and neuronal damage in the ischemic brain: the swiss knife in synaptic injury. Prog Neurobiol 143:1–35. https://doi.org/10.1016/j.pneurobio.2016.06.001

Dogan A, Celik I (2012) Hepatoprotective and antioxidant activities of grapeseeds against ethanol-induced oxidative stress in rats. Br J Nutr 107:45–51. https://doi.org/10.1017/S0007114511002650

Doyle KP, Simon RP, Stenzel-Poore MP (2008) Mechanisms of ischemic brain damage. Neuropharmacology 55:310–318. https://doi.org/10.1016/j.neuropharm.2008.01.005

Eichenbaum H (2004) Hippocampus: cognitive processes and neural representations that underlie declarative memory. Neuron 44:109–120. https://doi.org/10.1016/j.neuron.2004.08.028

El Kadmiri N, Cuardos R, El Moutawakil B et al (2014) A proteomic approach for the involvement of the GAPDH in Alzheimer disease in the blood of Moroccan FAD cases. J Mol Neurosci 54:774–779. https://doi.org/10.1007/s12031-014-0374-8

Fernandes J, Vieira M, Carreto L et al (2014) In vitro ischemia triggers a transcriptional response to down-regulate synaptic proteins in hippocampal neurons. PLoS One 9:e99958. https://doi.org/10.1371/journal.pone.0099958

Gancedo C, Flores C-L, Gancedo JM (2016) The expanding landscape of moonlighting proteins in yeasts. Microbiol Mol Biol Rev 80:765–777. https://doi.org/10.1128/MMBR.00012-16

Hoshino A, Helwig M, Rezaei S et al (2014) A novel function for proSAAS as an amyloid anti-aggregant in Alzheimer's disease. J Neurochem 128:419–430. https://doi.org/10.1111/jnc.12454

Huang DW, Sherman BT, Lempicki RA (2009) Bioinformatics enrichment tools: paths toward the comprehensive functional analysis of large gene lists. Nucleic Acids Res 37:1–13. https://doi.org/10.1093/nar/gkn923

Ikemoto A, Bole DG, Ueda T (2003) Glycolysis and glutamate accumulation into synaptic vesicles. Role of glyceraldehyde phosphate dehydrogenase and 3-phosphoglycerate kinase. J Biol Chem 278:5929–5940. https://doi.org/10.1074/jbc.M211617200

Institute of Laboratory Animal Resources (U.S.). Committee on Care and Use of Laboratory Animals., National Institutes of Health (U.S.). Division of Research Resources (1985) Guide for the care and use of laboratory animals

Jiang K, Yang C, Shui Q et al (2004) Time-course of mu-calpain activation, c-Fos, c-Jun, HSP70 and HSP27 expression in hypoxic-ischemic neonatal rat brain. Zhonghua Er Ke Za Zhi 42:441–445

Kadri S, Selima S, Mohamed E et al (2015) Protective effect of grape seed and skin extract on cerebral ischemia in rat: implication of transition metals. Int J Stroke 10:415–424. https://doi.org/10.1111/ijs.12391

Khazri O, Charradi K, Limam F et al (2016) Grape seed and skin extract protects against bleomycin-induced oxidative stress in rat lung. Biomed Pharmacother 81:242–249. https://doi.org/10.1016/j.biopha.2016.04.004

Laschet JJ, Minier F, Kurcewicz I et al (2004) Glyceraldehyde-3-phosphate dehydrogenase is a GABAA receptor kinase linking glycolysis to neuronal inhibition. J Neurosci 24:7614–7622. https://doi.org/10.1523/JNEUROSCI.0868-04.2004

Li SG, Ding YS, Niu Q et al (2015) Grape seed Proanthocyanidin extract alleviates arsenic-induced oxidative reproductive toxicity in male mice. Biomed Environ Sci 28:272–280. https://doi.org/10.3967/bes2015.038

Li M, Zhou Z-P, Sun M et al (2016) Reduced nicotinamide adenine dinucleotide phosphate, a pentose phosphate pathway product, might be a novel drug candidate for ischemic stroke. Stroke 47:187–195. https://doi.org/10.1161/STROKEAHA.115.009687

Lindsey ML, Mayr M, Gomes AV et al (2015) Transformative Impact of proteomics on cardiovascular health and disease: a scientific statement from the American Heart Association. Circulation 132:852–872. https://doi.org/10.1161/CIR.0000000000000226

Ma D, Zhang M, Mori Y et al (2010) Cellular localization of epidermal-type and brain-type fatty acid-binding proteins in adult hippocampus and their response to cerebral ischemia. Hippocampus 20:811–819. https://doi.org/10.1002/hipo.20682

Ma Y, Nie H, Chen H et al (2015) NAD^+/NADH metabolism and NAD^+-dependent enzymes in cell death and ischemic brain injury: current advances and therapeutic implications. Curr Med Chem 22:1239–1247

Manivannan J, Tay SSW, Ling E-A, Dheen ST (2013) Dihydropyrimidinase-like 3 regulates the inflammatory response of activated microglia. Neuroscience 253:40–54. https://doi.org/10.1016/j.neuroscience.2013.08.023

Margalef M, Pons Z, Bravo FI et al (2015) Tissue distribution of rat flavanol metabolites at different doses. J Nutr Biochem 26:987–995. https://doi.org/10.1016/j.jnutbio.2015.04.006

Marrif H, Juurlink BH (1999) Astrocytes respond to hypoxia by increasing glycolytic capacity. J Neurosci Res 57:255–260

Mele M, Aspromonte MC, Duarte CB (2016) Downregulation of GABAA receptor recycling mediated by HAP1 contributes to neuronal death in in vitro brain ischemia. Mol Neurobiol 54:45–57. https://doi.org/10.1007/s12035-015-9661-9

Mezni A, Aoua H, Khazri O et al (2017a) Lithium induced oxidative damage and inflammation in the rat's heart: protective effect of grape seed and skin extract. Biomed Pharmacother 95:1103–1111. https://doi.org/10.1016/j.biopha.2017.09.027

Mezni A, Khazri A, Khazri O et al (2017b) Neuroprotective activity of grape seed and skin extract against Lithium exposure using proteomic research. Mol Neurobiol 54:2720–2730. https://doi.org/10.1007/s12035-016-9853-y

Mokni M, Hamlaoui-Guesmi S, Amri M et al (2012) Grape seed and skin extract protects against acute chemotherapy toxicity induced by doxorubicin in rat heart. Cardiovasc Toxicol 12:158–165. https://doi.org/10.1007/s12012-012-9155-1

Nakajima H, Kubo T, Ihara H et al (2015) Nuclear-translocated Glyceraldehyde-3-phosphate dehydrogenase promotes poly(ADP-ribose) Polymerase-1 activation during oxidative/Nitrosative stress in stroke. J Biol Chem 290:14493–14503. https://doi.org/10.1074/jbc.M114.635607

Nassiri-Asl M, Hosseinzadeh H (2009) Review of the pharmacological effects of Vitis vinifera (Grape) and its bioactive compounds. Phytother Res 23:1197–1204. https://doi.org/10.1002/ptr.2761

Oudit GY, Trivieri MG, Khaper N et al (2006) Role of L-type Ca2+ channels in iron transport and iron-overload cardiomyopathy. J Mol Med 84:349–364. https://doi.org/10.1007/s00109-005-0029-x

Pacher P, Beckman JS, Liaudet L (2007) Nitric oxide and peroxynitrite in health and disease. Physiol Rev 87:315–424. https://doi.org/10.1152/physrev.00029.2006

Qvit N, Joshi AU, Cunningham AD et al (2016) Glyceraldehyde-3-phosphate dehydrogenase (GAPDH) protein-protein interaction inhibitor reveals a non-catalytic role for GAPDH oligomerization in cell death. J Biol Chem 291:13608–13621. https://doi.org/10.1074/jbc.M115.711630

Racay P, Matejovicová M, Drgová A et al (1998) The effect of ischemia and ischemia-reperfusion on ion transport systems. Bratisl Lek Listy 99:386–394

Rudinskiy N, Grishchuk Y, Vaslin A et al (2009) Calpain hydrolysis of alpha- and beta2-adaptins decreases clathrin-dependent endocytosis and may promote neurodegeneration. J Biol Chem 284:12447–12458. https://doi.org/10.1074/jbc.M804740200

Schafer DP, Jha S, Liu F et al (2009) Disruption of the axon initial segment cytoskeleton is a new mechanism for neuronal injury. J Neurosci 29:13242–13254. https://doi.org/10.1523/JNEUROSCI.3376-09.2009

Sehirli O, Ozel Y, Dulundu E et al (2008) Grape seed extract treatment reduces hepatic ischemia-reperfusion injury in rats. Phytother Res PTR 22:43–48. https://doi.org/10.1002/ptr.2256

Shannon P, Markiel A, Ozier O et al (2003) Cytoscape: a software environment for integrated models of biomolecular interaction networks. Genome Res 13:2498–2504. https://doi.org/10.1101/gr.1239303

Sharipov RR, Kotsiuruba AV, Kop″iak BS, Sahach VF (2014) Induction of nitrosative stress in mitochondria of rats hearts in experimental ischemia-reperfusion of the brain and its correction by ecdysterone. Fiziolohichnyĭ Zhurnal Kiev Ukr 1994 60:3–13

Shim SM, Lee WJ, Kim Y et al (2012) Role of S5b/PSMD5 in proteasome inhibition caused by TNF-α/NFκB in higher eukaryotes. Cell Rep 2:603–615. https://doi.org/10.1016/j.celrep.2012.07.013

Shyu W-C, Lin S-Z, Chiang M-F et al (2008) Secretoneurin promotes neuroprotection and neuronal plasticity via the Jak2/Stat3 pathway in murine models of stroke. J Clin Invest 118:133–148. https://doi.org/10.1172/JCI32723

Tanaka R, Mochizuki H, Suzuki A et al (2002) Induction of glyceraldehyde-3-phosphate dehydrogenase (GAPDH) expression in rat brain after focal ischemia/reperfusion. J Cereb Blood Flow Metab 22:280–288. https://doi.org/10.1097/00004647-200203000-00005

Turki K, Charradi K, Boukhalfa H et al (2016) Grape seed powder improves renal failure of chronic kidney disease patients. EXCLI J 15:424–433. https://doi.org/10.17179/excli2016-363

Ueda M, Muramatsu H, Kamiya T et al (2000) Pyruvate dehydrogenase activity and energy metabolite levels following bilateral common carotid artery occlusion in rat brain. Life Sci 67:821–826

Won SJ, Kim DY, Gwag BJ (2002) Cellular and molecular pathways of ischemic neuronal death. J Biochem Mol Biol 35:67–86

Yamashita T (2012) Ca2+−dependent regulation of synaptic vesicle endocytosis. Neurosci Res 73:1–7. https://doi.org/10.1016/j.neures.2012.02.012

Zhai D, Chin K, Wang M, Liu F (2014) Disruption of the nuclear p53-GAPDH complex protects against ischemia-induced neuronal damage. Mol Brain 7:20. https://doi.org/10.1186/1756-6606-7-20

Zhang G, Wang F, Geng M, Chen L (2011) Comparative proteomic analysis of hippocampus between chronic cerebral ischemia rats and normal controls. Zhong Nan Da Xue Xue Bao Yi Xue Ban 36:992–998. https://doi.org/10.3969/j.issn.1672-7347.2011.10.010

Zhang R, Tang S, Huang W et al (2015) Protection of the brain following cerebral ischemia through the attenuation of PARP-1-induced neurovascular unit damage in rats. Brain Res 1624:9–18. https://doi.org/10.1016/j.brainres.2015.07.023